

# Structural characteristics and magnetic properties of $\lambda$ - $\text{MnO}_2$ films grown by plasma-assisted molecular beam epitaxy

L. W. Guo<sup>a)</sup>

*Institute of Physics, Chinese Academy of Sciences, Beijing 100080, China*

D. L. Peng, H. Makino, T. Hanada, S. K. Hong, K. Sumiyama, and T. Yao

*Institute for Materials Research, Tohoku University, Sendai, Japan*

K. Inaba

*X-Ray Research Laboratory, Rigaku Corporation, Tokyo, Japan*

(Received 3 October 2000; accepted for publication 26 March 2001)

High-quality  $\lambda$ - $\text{MnO}_2$  single-crystal films were fabricated on MgO (001) substrates by plasma-assisted molecular beam epitaxy. The structural characteristics and magnetic properties of the films were studied. Two magnetic transition temperatures, T1 and T2, were observed from the films. Their magnetic behavior differed from that of bulk polycrystalline samples synthesized by removing Li ions from the parent  $\text{LiMn}_2\text{O}_4$ . The first, T1, setting at around 20 K, corresponded to long-range antiferromagnetic ordering similar to that observed in bulk at 32 K. T2, set at 43 K, corresponded to weak long-range ferromagnetic ordering among net magnetization of clusters, in which short-range antiferromagnetic ordering existed. T1 shifted to lower temperature with decreasing film thickness, which indicated that the proximity of the interface and strain played a key role in determining the transition temperature. © 2001 American Institute of Physics.

[DOI: 10.1063/1.1377303]

## I. INTRODUCTION

Since Hunter<sup>1</sup> reported that  $\lambda$ - $\text{MnO}_2$ , a phase of Mn oxides, could be prepared by removing Li ions from spinel  $\text{LiMn}_2\text{O}_4$  while retaining the structure of the parent phase, only a few articles have been reported on the structural, electrochemical, and magnetic properties of bulk spinel  $\lambda$ - $\text{MnO}_2$ .<sup>2-5</sup> In spinel structure, Mn ions occupy the octahedral sites and their magnetic sublattice consists of a pyrochlore-type array of corner-shared tetrahedral, which is an ideal candidate for geometrical frustrated magnetic structures.<sup>6-8</sup> However, all of these reported  $\lambda$ - $\text{MnO}_2$  samples were synthesized by electrochemical delithiation or acid leaching, where some of the Li ions remained in the samples. Consequently, some of the inherent properties of the pure  $\lambda$ - $\text{MnO}_2$  structure might be modified by Li ions or induced  $\text{Mn}^{3+}$  ions. Meanwhile, it is unclear whether the spinel  $\lambda$ - $\text{MnO}_2$  can be stabilized without Li ions. Hence, fabricating high-quality  $\lambda$ - $\text{MnO}_2$  single crystals or films is needed to clarify intrinsic magnetic characteristics and to explore possible applications. In the present article, plasma-assisted molecular beam epitaxy (MBE) was used to grow  $\lambda$ - $\text{MnO}_2$  high-quality single-crystal films for studies of their structure and magnetic properties. Meanwhile, a comparison of their magnetic properties with bulk polycrystalline samples prepared by Li ion removal is also given.

## II. EXPERIMENT

$\lambda$ - $\text{MnO}_2$  films were grown on MgO (001) substrates by plasma-assisted MBE under well-controlled growth condi-

tions. Since MBE relies on nonequilibrium thermodynamic processes, the growth of materials in a metastable phase is facilitated by careful control of growth conditions. By reducing the growth rate to less than 2 nm/min, high-quality  $\lambda$ - $\text{MnO}_2$  single-crystal films were grown on MgO (001) substrates. The detailed preparing of MgO substrate and growth process of Mn oxides were described elsewhere.<sup>9</sup> The structural properties and surface morphology of  $\lambda$ - $\text{MnO}_2$  films were characterized by x-ray diffraction (XRD), extended x-ray absorption fine structure (EXAFS) and atomic force microscopy (AFM). Magnetic properties of the films were measured using a superconducting quantum interference device magnetometer. Magnetic field applied parallel to the growth plane of the films.

## III. RESULTS AND DISCUSSION

The XRD patterns of the films suggest that the films are single crystals with a face-centered cubic structure. The lattice constant is estimated to be about 8.4 Å (nearly twice of the MgO substrate). The films are [001] oriented with the [100] (or [010]) axis being parallel to the [100] (or [010]) axis of the MgO substrate, if a unit cell of face-centered cubic lattice is adopted. The EXAFS result showed that the Mn *K*-edge absorption curve of the film was similar to that of  $\text{LiMn}_2\text{O}_4$ . However, the absorption edge of  $\lambda$ - $\text{MnO}_2$  film shifted slightly to higher energy compared with that of the  $\text{LiMn}_2\text{O}_4$  reference sample. The observed higher absorption edge in the  $\lambda$ - $\text{MnO}_2$  film is consistent with the higher chemical valence of its constituent Mn ions ( $\text{Mn}^{+4}$ ) than that ( $\text{Mn}^{+3.5}$ ) in  $\text{LiMn}_2\text{O}_4$ , since position of absorption edge correlates closely with the average effective charge on the Mn ions. However, it should be noted that the lattice constant of

<sup>a)</sup> Author to whom correspondence should be addressed: electronic mail: lwguo@aphy.iphy.ac.cn

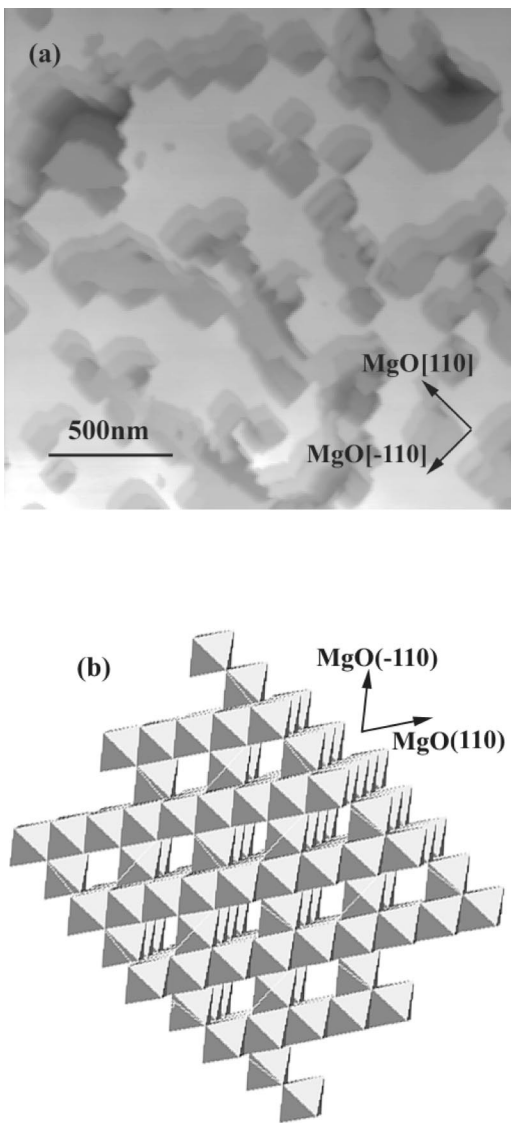


FIG. 1. (a) AFM images of a  $\lambda$ - $\text{MnO}_2$  film, where the edges of pits are parallel to the [110] or [-110] directions of MgO substrate. (b) Schematic representation of a spinel  $\lambda$ - $\text{MnO}_2$  structure, where edge-shared octahedral forms a chain-shaped arrangement along [110] or [-110] direction of MgO substrate.

the film was 4.3% larger than that of bulk crystal, 8.04 Å. It is likely that the film is strained due to lattice mismatch with the MgO substrate, since the film thickness ranging from 100 to 400 nm is not thick enough to relax the whole strain. For all of the  $\lambda$ - $\text{MnO}_2$  films, their surface was flat. However, some of the films contained pits on the surface, as shown in Fig. 1(a). It is seen that the edges of the pits are all parallel to either the [110] or [-110] direction of the MgO substrate, which reflects the inherent structure of  $\lambda$ - $\text{MnO}_2$ . In  $\lambda$ - $\text{MnO}_2$  structure, the sublattice of oxygen atoms forms an edge-shared octahedron arrangement which results in a chain-shaped array in the (001) plane as schematically depicted in Fig. 1(b). Note that the chains are aligned along the [110] (or [-110]) of MgO. Since the atomic bonding between different chains is weak, the pits begin to form once the bonds are broken. Figures 1(a) and 1(b) indicate that the surface morphology is closely dependent on the crystal structure.

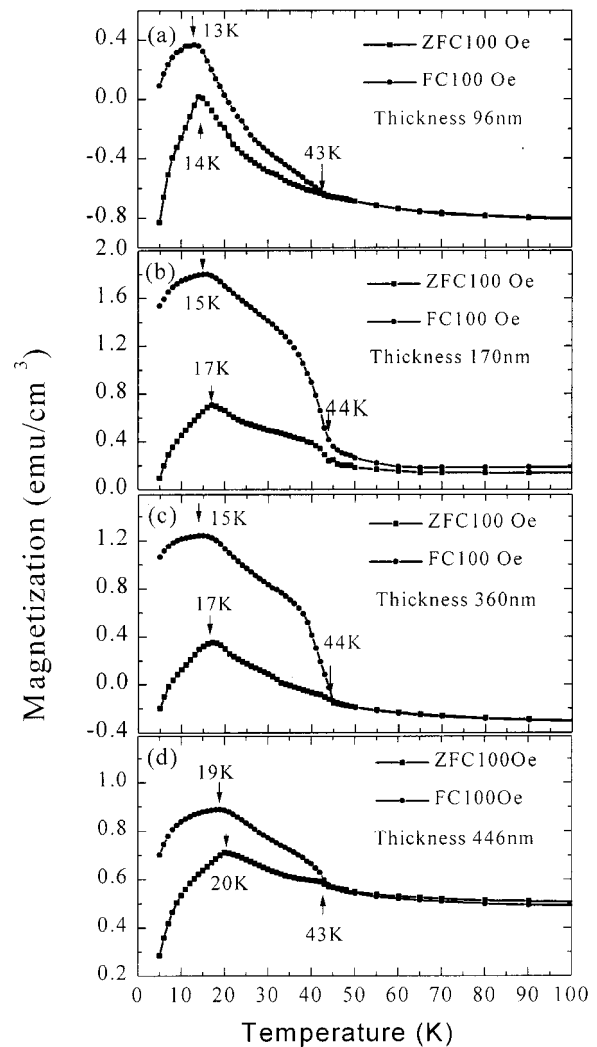


FIG. 2. Temperature dependence of magnetization on FC and ZFC runs for different film thickness, (a) 96, (b) 170, (c) 360, and (d) 446 nm.

Besides the structural characteristics of  $\lambda$ - $\text{MnO}_2$  films, their magnetic properties were studied. Magnetization of the films was measured during warm up under the different cooling conditions of field cooled (FC) and zero field cooled (ZFC). Figure 2 shows the dependence of the magnetization on temperature for various film thicknesses. The purity of the MgO substrate was such an impurity concentration 0.01% that small amounts of magnetic impurities might be contained. The magnetization contribution from the MgO substrate should be eliminated. Therefore, the magnetization data from the film were corrected by subtracting the magnetization of a MgO substrate with the same surface area as the film. As shown in Fig. 2, the resultant magnetization of the films becomes minus or smaller at low temperature compared with that at high temperature paramagnetic part. The feature becomes obvious even in thinner films. We suppose it is induced by unrefined subtracting substrate magnetization due to different magnetization behaviors in MgO substrates before and after epitaxy. However, no matter what the absolute magnetization value is, two significant features can be observed in Fig. 2: the cusp located at 14–20 K (denoted as T1) and the divergence point at 43 K (denoted as T2) in both

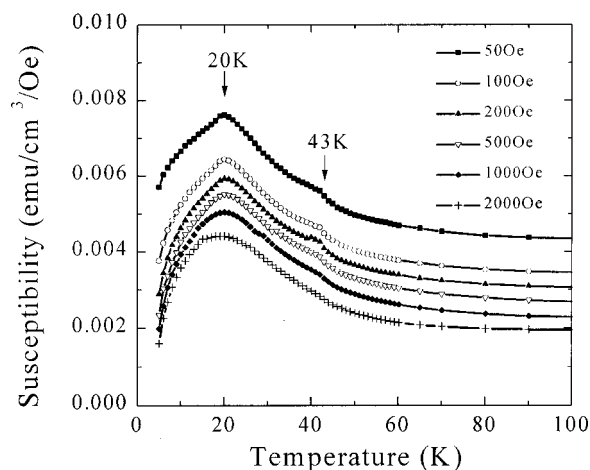


FIG. 3. Susceptibility data of a 446 nm film at different applied fields under ZFC run. The inflection at  $T_2$  (43 K) is not clear at a 2000 Oe field.

the ZFC and FC magnetization. In the following, the cusp behavior is discussed first.

As the film thickness increased from (a) to (d) in Fig. 2,  $T_{1ZFC}(T_{1FC})$  for ZFC (FC) run increased also from 14 (13)–20 K (19 K), that is similar to the phenomena usually observed in magnetic metal films<sup>7,8</sup> due to the effects of interface and strain. In Fig. 2, three magnetization regions are seen clearly: region I,  $T < T_1$ , region II,  $T_1 < T < T_2$ , and region III,  $T > T_2$ . In region I, both FC and ZFC magnetization drop rapidly with lowering temperature, showing a typical feature of long-range antiferromagnetic ordering. This feature is similar to the behavior of the bulk polycrystalline sample, where the electronic spin arrangement is not a simple up and down and its spin unit cell is twice of the lattice unit cell.<sup>2</sup> However, the  $T_1$  (14–20 K) of the films was lower than that observed in bulk polycrystal at 32 K, which may be due to stronger exchange interactions between Mn ions in bulk. As mentioned above, lattice constant 8.04 Å of an acid leached bulk sample<sup>2</sup> is smaller than 8.4 Å of the films, which results in a stronger magnetic interaction among the nearest Mn ions in bulk than in the films. To understand the dependence of the cusp feature on applied field, the susceptibility of a 446 nm thick film corresponding to the sample of Fig. 2(d) is measured in ZFC, as shown in Fig. 3. The sharp cusp was maintained up to a field of 500 Oe. Under higher field, the cusp becomes broad and its center shifted from 20 K at 500 Oe to 19 K at 2000 Oe. In addition, an inflective point at  $T_2$  is discernible up to a field of 1000 Oe. The close dependence of susceptibility on applied fields suggests that there is a strong field-induced magnetic anisotropy in the  $\lambda$ - $MnO_2$  films. Evidence to support this inference is found in its magnetization hysteresis curves. The detailed studies of magnetization hysteresis behaviors at different temperature will be published elsewhere.

Besides the  $T_1$ , the  $T_2$  is observed in the  $\lambda$ - $MnO_2$  film, which has never been observed in bulk polycrystalline  $\lambda$ - $MnO_2$ . As seen in Fig. 2, when temperature is in region I, the magnetic interaction of Mn ions is a long-range antiferromagnetic one. When temperature is in region III, the magnetic interaction is a paramagnetic one and the magnetization

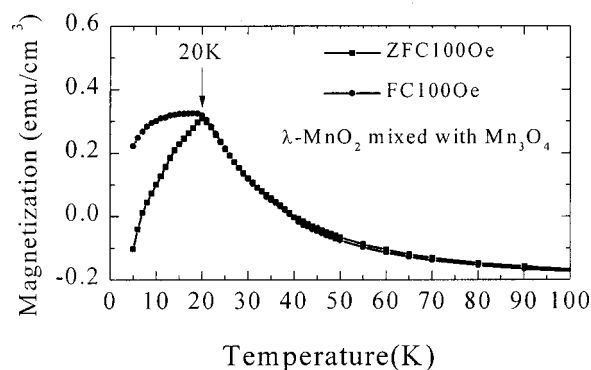


FIG. 4. Temperature dependence of the magnetization on FC and ZFC runs for a 375 nm  $\lambda$ - $MnO_2$  film mixed with small amounts of  $Mn_3O_4$  phase.

of ZFC and FC overlaps. Therefore, it is reasonable to infer that region II should be a transition region for a short-range antiferromagnetic ordering developed to a long-range one. When temperature varied from  $T_2$  to  $T_1$ , the size of the clusters with short-range antiferromagnetic ordering would develop in expending of the paramagnetic parts. In Fig. 2(b) and 2(c), an abrupt increase in magnetization is seen clearly in the FC run. This indicates a weak long-range ferromagnetic interaction appearing among the clusters, in which a short-range antiferromagnetic ordering might be still existed due to the canting arrangements of the net spins in the cluster.<sup>10</sup> The situation is similar to the magnetic behavior in  $Mn_3O_4$  structure, since they contain the same octahedral-site Mn atoms. Therefore, we inferred that  $T_2$  is a magnetic transition temperature for the onset of a short-range antiferromagnetic ordering and also for a weak long-range ferromagnetic interaction among clusters. But, it should be pointed out that the short-range antiferromagnetic ordering in  $\lambda$ - $MnO_2$  film should not be a simple spin up and down arrangement owing to a strong interaction among Mn ions whose sublattice is composed of a tetrahedral type arrangement, which is a typical geometry frustrated configuration.

Here, it should be explained why the  $T_2$  is observed only in  $\lambda$ - $MnO_2$  single-crystal films. As well known, if a magnetization process depends on its cooling history, there must exist a long-range field-induced magnetic anisotropy. In polycrystalline sample, there is no long-range crystalline ordering owing to the disorder of crystal orientation among grains. Therefore, the  $T_2$ , related to a weak long-range ferromagnetic ordering, cannot be observed in polycrystalline sample. This conjecture is supported by an experimental result from one of our samples in which a small amount of  $Mn_3O_4$  phase was mixed in the  $\lambda$ - $MnO_2$  structure. Figure 4 showed the magnetization curve of this sample under ZFC and FC cooling run. It is noted that a cusp ( $T_1=20$  K) is observed only, and the magnetization for ZFC and FC diverges at the cusp. This is very similar to the results of polycrystalline samples synthesized by acid leaching.<sup>2</sup> Because long-range crystalline ordering is destroyed in this mixed phase sample, its structural characteristic is similar to that of a polycrystalline sample. Therefore, it can be well understood that why the  $T_2$  has not been observed in polycrystalline samples.

#### IV. CONCLUSIONS

In summary, high-quality  $\lambda$ -MnO<sub>2</sub> single-crystal films have been fabricated on MgO (001) substrates by plasma-assisted MBE. Two magnetic transition temperatures, T1 and T2, are observed in the  $\lambda$ -MnO<sub>2</sub> single-crystal films. T1 is a magnetic transition temperature for a long-range antiferromagnetic ordering. T1 has a close correlation with strain and interface. T2 is a magnetic transition temperature for the onset of a weak long-range ferromagnetic ordering among clusters with short-range antiferromagnetic ordering. Our experiments demonstrate that a metastable structure can be realized using MBE by choosing a suitable substrate and well controlled growth conditions. Meanwhile, it reveals studies of high-quality single-crystal films will disclose more inherent magnetic characteristics in the structure.

#### ACKNOWLEDGMENTS

One of the authors (L.W.G.) would like to give her thanks to Dr. H. L. Bai and Dr. Y. Nakanishi for their helpful discussions.

<sup>1</sup>J. C. Hunter, *Solid State Chem.* **39**, 142 (1981).

<sup>2</sup>J. E. Greedan, N. P. Raju, A. S. Wills, C. Morin, and S. M. Shaw, *Chem. Mater.* **10**, 3058 (1998).

<sup>3</sup>D. Larcher, P. Courjal, R. Herrera Urbina, B. Gerand, A. Blyr, A. du Pasquier, and J. M. Tarascon, *J. Electrochem. Soc.* **145**, 3392 (1998).

<sup>4</sup>M. M. Thackeray, P. J. Johnson, L. A. de Picciotto, P. G. Bruce, and J. B. Goodenough, *Mater. Res. Bull.* **19**, 179 (1984).

<sup>5</sup>T. J. Richardson and P. N. Ross, *Mater. Res. Bull.* **31**, 935 (1996).

<sup>6</sup>A. P. Ramirez, *Annu. Rev. Mater. Sci.* **24**, 453 (1994).

<sup>7</sup>B. D. Gaulin, J. N. Reimers, T. E. Mason, J. E. Greedan, and T. Tun, *Phys. Rev. Lett.* **69**, 3244 (1992).

<sup>8</sup>J. N. Reimers, J. E. Greedan, R. K. Kremer, E. Gmelin, and M. A. Subramanian, *Phys. Rev. B* **43**, 3387 (1991).

<sup>9</sup>L. W. Guo, H. J. Ko, D. H. Makino, Y. F. Chen, K. Inaba, and T. Yao, *J. Cryst. Growth* **205**, 531 (1999).

<sup>10</sup>T. Moriya, in *Magnetism*, Vol. I, edited by G. T. Rado and H. Suhl (Academic, New York, 1963), p. 85.